Evidence for symmetric cationic sites in zirconium-bearing oxide glasses

G. Ferlat, L. Cormier, M. H. Thibault, L. Galoisy, and G. Calas
Institut de Minéralogie et de Physique des Milieux Condensés, UMR CNRS-IPGP-Universités Paris 6 et 7 No. 7590, case 115, 4 place Jussieu, 75252 Paris cedex 05, France

J. M. Delaye and D. Ghaleb
Commissariat à l'Énergie Atomique (CEA), Centre de la vallée du Rhône, Marcoule, DEN/DTCD/SECM/LCLT, BP 171, 30207 Bagnols-sur-Cèze cedex, France

(Received 5 October 2005; revised manuscript received 23 March 2006; published 23 June 2006)

The local environment of Zr in a borosilicate glass has been investigated by combining molecular dynamics (MD) simulations with Zr *K*-edge x-ray absorption spectroscopy (XAS) measurements. Two- and three-body distribution functions in agreement with the experimental data were obtained. The oxygen first neighbors around Zr are found to be narrowly distributed, revealing almost perfectly regular ZrO_6 octahedra. Significant three-body contributions (Zr-O-O) to the XAS signal are observed, probing the existence of highly symmetric cationic sites in a glassy network. The $g_{ZrO}(r)$ first peak derived from the experimental data is narrower than the one given by the MD model, thus providing elements for further improvements of the MD potentials.

DOI: 10.1103/PhysRevB.73.214207 PACS number(s): 61.10.Ht, 61.43.Fs, 02.70.Ns

I. INTRODUCTION

Oxide glasses such as borosilicates are materials of technological interest (e.g., for coatings, waste confinement) as well as challenging systems from the point of view of their structural description.[1]

The structure of oxide glasses is commonly described by the coexistence of a polymeric network made of rigid units (e.g., silicate tetrahedra) and of cations which may act either as modifying elements breaking the connectivity of the network, or as charge-compensating cations balancing local charge deficits.[2–4] The presence of cations acting as network formers and modifiers can have drastic effects on the chemical durability and the mechanical characteristics of the glass. Whether the zirconium ion acts as a network former or as a modifier is still a matter of debate (it is sometimes classified as intermediate[5]) since a versatile behavior is observed. Adding ZrO_2 oxide imparts increase in density, viscosity, liquidus temperature, mechanical and chemical resistance, electrical conductivity, and decrease in thermal expansion coefficient.[6,7] In glass ceramics containing only a minor amount of ZrO_2, Zr is acting as a nucleating agent.[8] This versatile behavior demonstrates that zirconium ion plays a paramount role in the glasses' structure. However, the correlations between the structural modifications and the final glass macroscopic properties are poorly understood.

There have been several works aimed at determining the local environment of Zr in glasses by means of x-ray absorption spectroscopy[5,9–11] (XAS). It was obtained, in particular from x-ray absorption near edge structure (XANES) measurements at $L_{2,3}$ edge,[10] that Zr sits in octahedral ZrO_6 sites. The analysis of the extended x-ray absorption fine structure (EXAFS) *K*-edge data also revealed the presence of contributions arising from long scattering paths, which were attributed to second shells of neighbors.[10,11] However, the quantitative determination of these neighboring shells from the EXAFS data alone was not possible due to the large number of possible solutions (Na, Si, B, etc.), all these shells being expected to overlap in the same region (in between 3.4 and 4.0 Å). Using bond-valence rules, it was, however, predicted that charge-compensating cations (such as Na^+, Ca^{2+}) would stabilize the $(ZrO_6)^{2-}$ octahedra.[10]

In this paper, the local structure of Zr in a borosilicate glass is addressed. The glass composition corresponds to a simplified glass model for nuclear waste storage (similar compositions were studied in Refs. 12–14). Using a methodology that combines EXAFS with molecular dynamics (MD) simulations, the present work aims at overcoming some of the limitations encountered in the previous studies. While there have been several attempts to model zirconium bearing glasses by MD simulations,[15,16] this work directly confronts the theoretical results, regarding the Zr local structure, to experimental data. Evidence for regular octahedral Zr sites will be presented, adding support to the *network formerlike* behavior of zirconium in such glasses.

II. EXPERIMENTAL AND MD SIMULATION DETAILS

A glass of composition (mol %) 41.7 SiO_2 – 5.13 Al_2O_3 – 28.49 B_2O_3 – 20.08 Na_2O – 4.6 ZrO_2 was prepared by mixing the appropriate amounts of SiO_2, Al_2O_3, H_3BO_3, Na_2CO_3, and ZrO_2 powders. After melting at 1100 °C in a platinum crucible, the sample was poured and annealed at 520 °C for 1 h. Glass composition and homogeneity were checked by electron microprobe analysis using a Cameca SX50 Microbeam.

X-ray absorption (XAS) spectra were acquired at the D44 beamline at the Laboratoire pour l'Utilisation du Rayonnement Electromagnétique, Orsay, France working in transmission mode at the Zr *K*-edge (17 998 eV). Three XAS spectra were recorded at 10 K. More details on the sample preparation and data acquisition can be found elsewhere.[10] Extended x-ray absorption fine structure (EXAFS) oscillations were extracted using the GNXAS package.[17,18] The absorption background in the energy range 18 018 – 19 200 eV was modeled by three polynomial splines. Since the presence of multi-electron excitation channels in the atomic background

TABLE I. Composition of the simulated glass (mol %).

SiO_2	B_2O_3	Na_2O	Al_2O_3	ZrO_2
40	30	20	5	5

of fifth-period elements has been reported,[19] a step-shaped function was used to empirically model the $KM_{4,5}$ excitation (near 18 200 eV).

The molecular dynamics procedure used to investigate the glass structure has been presented in previous papers[12–14] and only a brief account will be given below. Empirical force fields of Born-Mayer-Huggins type were employed to describe the interatomic interactions with parameters used in previous studies of similar systems.[12–14] Three-body potentials were applied to O-Si-O, O-B-O and Si-O-Si triplets in order to impose a local angular order consistent with experimental data; these terms were developed in previous works.[20] For the Zr-O pair potential, the values used for ϵ and σ are 4619.22 eV and 0.29 Å, respectively.

The system is made of 2400 atoms with a composition close to the experimental one (see Table I). Simulations were carried out in the microcanonical ensemble using a cubic box of 29.944 Å and a time step of 1 fs. The edge of the cell is adjusted so as to anneal the internal pressure: it corresponds to a final density of 2.75 g cm^{-3}. The liquid is first equilibrated at 5000 K during 5 ps, then the temperature is cooled to 293 K at a rate of 4×10^{14} K s^{-1}. A final relaxation at ambient temperature is performed during 65 ps and the radial distribution functions are averaged on the last 6 ps.

III. RESULTS AND DISCUSSION

A. MD simulations

The average atomic structure seen from a given atom can be described using *n-body* distribution functions g_n. In particular, the g_2 functions, usually called partial radial distribution functions (PRDF) and hereafter noted $g_{\alpha\beta}(r)$, are normalized histograms of interatomic distances involving the α and β species. Similarly, $g_3(r_1,r_2,\theta)$ functions are triplet distribution functions (i.e., three-dimensional normalized histograms of interatomic angles).

The partial radial distribution functions (PRDF) $g_{ZrX}(r)$ obtained from the MD simulations are shown Fig. 1, left panel, together with the corresponding running coordination numbers, $n_{ZrX}(r)$, right panel. A pronounced first peak at about 2.1 Å is visible in the $g_{ZrO}(r)$; the value of $n_{ZrO}(r)$ at 3.0 Å is 6. It thus appears that Zr sits in octahedral sites, as found in previous studies of similar glasses.[9–11,15] The shape of the $g_{ZrO}(r)$ first peak is similar (i.e., asymmetric at high-r values) to the one obtained in a previous MD study of similar glasses.[15] However, a significant difference is obtained regarding the position of the first maximum: about ~1.95 Å in Ref. 15 as compared to ~2.1 Å in the present case. This latter value is in good agreement with the Zr-O mean distance (2.07–2.10 Å) derived from previous EXAFS studies.[5,9–11]

All other ZrX (X=Si,B,Na,Al,Zr) PRDF show less structured peaks in the 3–4 Å range. Note that the total number of network-former ions (Si, B, Al) at 3.8 Å is close to 6 (6.7). This number, as well as the positions of the peaks in the PRDF, indicate that, on average, each oxygen of the ZrO_6 octahedra (see Table II) is corner shared with the polyhedra which constitute the polymeric network. About three Na atoms are observed in the surrounding of Zr, as expected to ensure charge compensation of the Zr octahedral sites.

B. Combining MD with EXAFS: Spectra from the MD $g(r)$

The *n-body* distribution functions obtained from the MD simulations can be used to generate *synthetic* EXAFS spec-

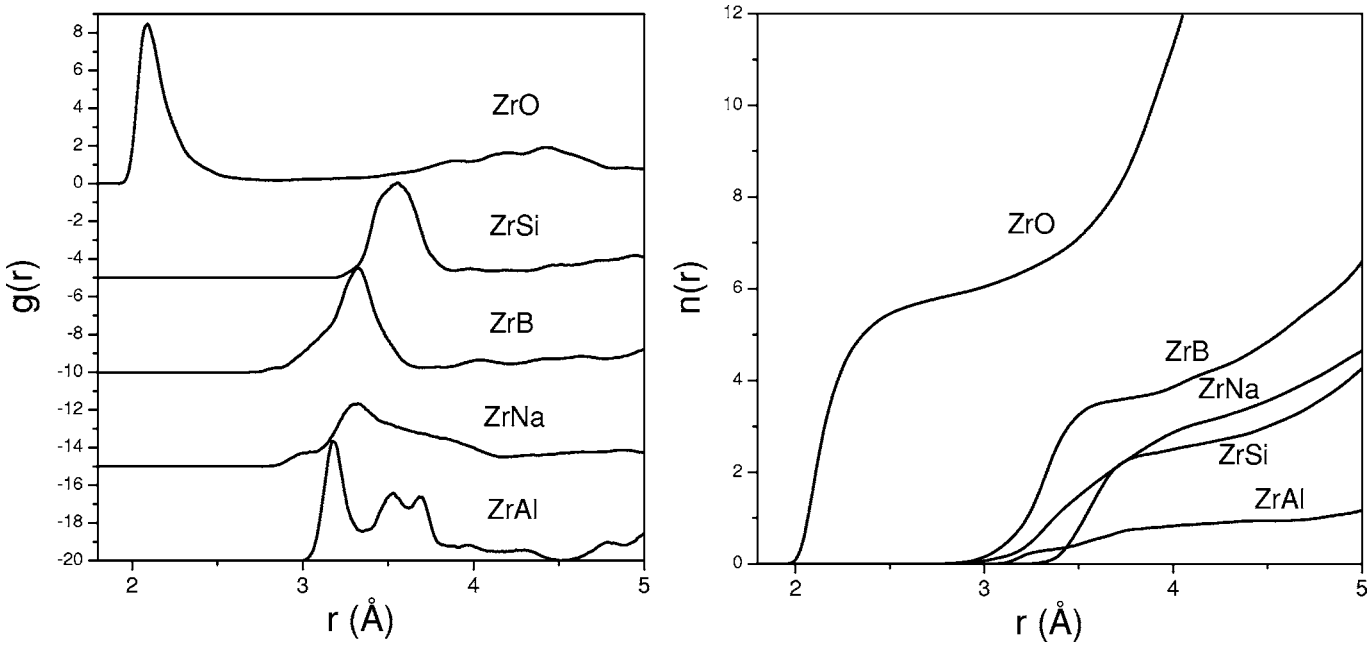

FIG. 1. Left panel: Zr-X (X=O,Si,B,Al,Na) partial radial distribution functions obtained from the MD simulation. The data are shifted vertically for clarity. Right panel: corresponding running coordination numbers $n_{ZrX}(r)$ (obtained from $n_{ZrX}(r)=4\pi\rho_X\int_0^r g_{ZrX}(r')r'^2dr'$).

TABLE II. Partial N_{ZrX} coordination numbers obtained from the value of the running coordination number at R_{ZrX} (given in bracket).

N_{ZrO}(3.0 Å)	N_{ZrSi}(3.8 Å)	N_{ZrB}(3.8 Å)	N_{ZrAl}(3.3 Å)	N_{ZrNa}(4.2 Å)
6	2.3	3.6	0.3	3.2

tra. For a monoatomic system, the EXAFS signal is given by[21]

$$\langle \chi(k) \rangle = \int dr 4\pi\rho r^2 g_2(r) \gamma^{(2)}(k,r) + \int dr_1 dr_2 d\theta 8\pi^2 r_1^2 r_2^2 \sin(\theta) \rho^2 g_3(r_1, r_2, \theta) \times \gamma^{(3)}(r_1, r_2, \theta, k) + \ldots, \quad (1)$$

where ρ is the number density and the $\gamma^{(n)}$ functions are the irreducible n-body contributions[18] to the EXAFS signal (contributions from n higher than 3 have been omitted). Thus, the first term in Eq. (1) stands for all possible scattering contributions (single and multiple scatterings) involving the absorber and one scatterer, the second term represents multiple-scattering contributions involving the absorber and two scatterers, etc.

For a multicomponent system, the first term on the right hand side of Eq. (1) must be replaced by a summation running over all possible pairs $(\alpha\beta)$ involving the x-ray absorbing species α

$$\sum_{(\alpha\beta)} \int_0^{r_{\alpha\beta}} 4\pi\rho_\beta r^2 g_{\alpha\beta}(r) \gamma^{(2)}_{\alpha\beta}(k,r) dr, \quad (2)$$

where $\gamma^{(2)}_{\alpha\beta}(k,r)$ is the EXAFS signal corresponding to a single atom pair at distance r. Similarly, the second term on the right hand side of Eq. (1) must be replaced by a summation running over all possible triplets involving the x-ray absorbing species α. See Refs. 21 and 22 and references therein for more details.

The GNXAS package has been used to compute the n-body contributions to the EXAFS signal at the Zr K edge. Zr-X two-body contributions were obtained using in Eq. (2) the MD PRDF shown in Fig. 1. These contributions are presented, together with the total two-body EXAFS signal hereby obtained, in Fig. 2. The Zr-O partial signal is by far the dominant one. Although smaller, Zr-Si and Zr-B ones are significant, whereas Zr-Na, Zr-Al are negligible (Zr-Zr, not shown, was fully neglected).

Figure 2 evidences the effective EXAFS contribution from each type of neighbor (and thus provides clues to guess which type of species is likely to be detected in the experimental signal). Although these signals were calculated from PRDF which may be improved (see next paragraphs), we believe that one can still gain information on the relative importance of each contribution: whereas the number of neighbors (up to 5 Å, see Fig. 1, right panel) decreases in the order $O > B > Na > Si > Al$, it appears that the effective EXAFS contribution in k space (Fig. 2) decreases in the order $O > Si \simeq B > Na > Al$, due to the atomic characteristics (x-ray scattering amplitude and phase functions) entering in the expression of $\gamma^{(2)}_{\alpha\beta}(k,r)$ [Eq. (2)].

The comparison of the calculated and experimental spectra shows a qualitative agreement (Fig. 2). However, it is obvious from the strong residual obtained that some of the Zr-X contributions are miscalculated (due to inaccuracies in the MD PRDF). The position of the peaks in the residual signal indicates that the main source of error should come from the Zr-O signal. As shown in the next section, higher-order correlations must be included in order to obtain a flat residual in the range 3–5 $Å^{-1}$.

C. Toward a refined model

Following the methodology of Ref. 23, a structural model compatible with the experimental EXAFS spectra can be retrieved using the MD $g(r)$ as an input model in a refinement process. This methodology consists in a decomposition of the initial $g(r)$ into several (usually one or two) short-range peaks plus a *tail* [long-range part of the $g(r)$]. The parameters which describe the short-range peaks can then be varied in a fitting process while keeping the long-range contribution fixed.[23] In this way, the refinement of the short-range part (to which EXAFS is very sensitive) is anchored on a realistic description of the long-range part (to which EXAFS is almost blind), provided by the initial model.

In the case of a monoatomic system, the refinement can be further constrained by imposing the reconstructed model

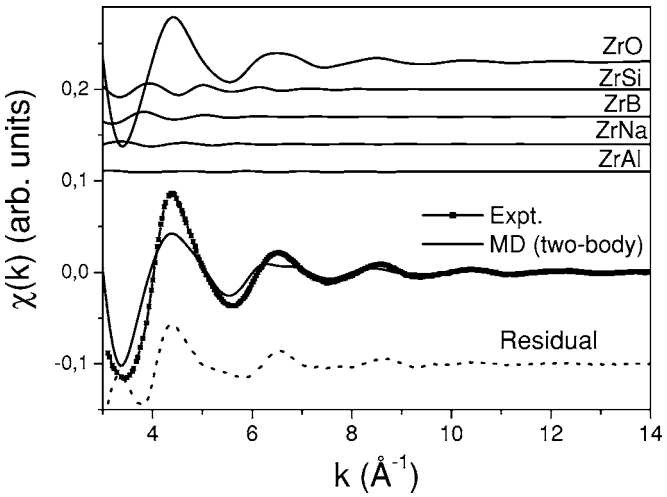

FIG. 2. Zr-X (X=O,Si,B,Al,Na) partial EXAFS signals calculated from the MD PRDF (Fig. 1) using Eq. (2). The signals are shifted up vertically for clarity. Comparison of the total two-body calculated signal (solid line) with the experimental spectrum (line +symbol). The residual (dots) is shifted down vertically.

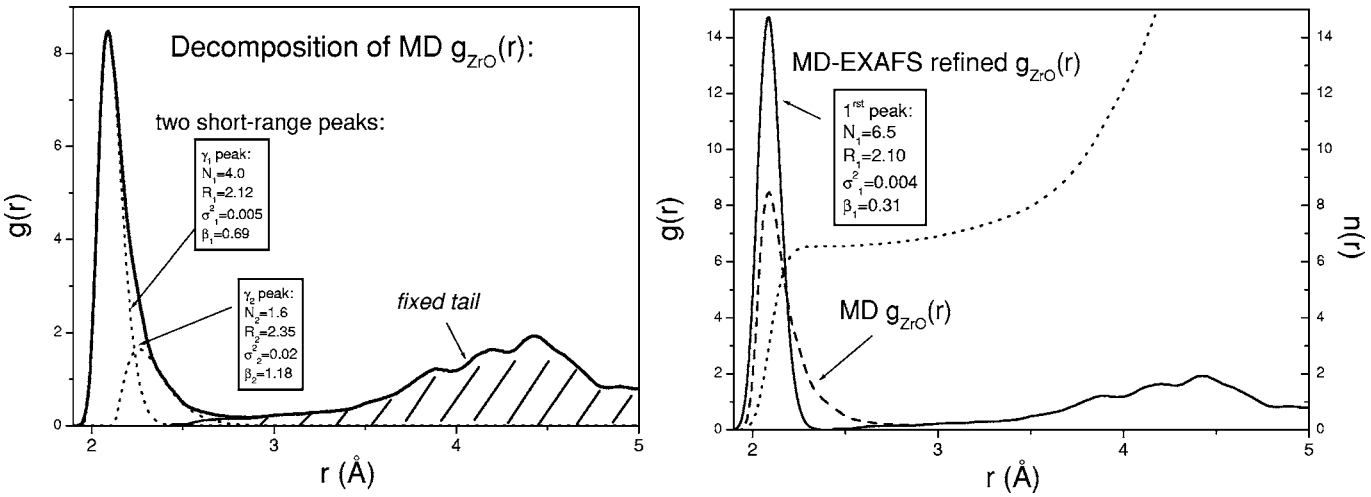

FIG. 3. Left panel: decomposition of the model $g_{ZrO}(r)$ partial radial distribution function into short-range γ-like peaks (dashed curved) and a long-range tail (open symbols). Right panel: reconstructed $g_{ZrO}(r)$ (solid line) after refinement of the short-range peaks of the MD model, together with the original MD model (dashed line). The reconstructed $g_{ZrO}(r)$ is shown with dots. The values for N, R, σ, and β refer to the parameters used in the analytical representation of the γ peaks (Ref. 23).

to obey the compressibility sum rule.[24] This methodology has been recently extended to the case of binary systems.[25] However, we did not make use of these constraints for our multi-component system.

Since the ZrO contribution is prevailing (see Figs. 2 and 5), it is essential to allow for the refinement of the $g_{ZrO}(r)$ PRDF. To this end, the low-r part of $g_{ZrO}(r)$ has been fitted by two asymmetric peaks (γ-like functions[23]); the remaining long-range part is hereafter called the *tail*: this decomposition is shown in Fig. 3, left panel. Each of these contributions (peaks plus tail) is used to generate the total EXAFS spectrum corresponding to this input structural model. The parameters describing the low-r peaks are then adjusted (while the tail contribution is kept fixed) until the residual between the experimental and calculated EXAFS spectra and the experimental one is small enough (below the experimental variance). The $g_{ZrSi}(r)$ and $g_{ZrB}(r)$ were also modeled by one γ peak and a remaining tail; however, the sensitivity on these contributions is too low to contribute significantly to the fit. The ZrNa contribution was fixed to its original value and the ZrAl one was neglected.

The best agreement obtained using two-body signals only is shown in Fig. 4 while in Fig. 5, both two- and three-body contributions were included simultaneously. The three-body contributions were restricted to two O-Zr-O angular distributions centered on 90 and 180°.[26] As can be seen in Figs. 4 and 5, the agreement between the calculated and experimental signals has been drastically improved. This results in a narrowing of the $g_{ZrO}(r)$ first peak: its amplitude is increased while its shape is more symmetric than the original MD model (see Fig. 3, right panel). This indicates that the Zr environment corresponds to almost regular octahedra.

A noticeable result is given by the presence of a marked high frequency residual between the experimental and the (refined) calculated spectra using two-body contributions only (Fig. 4). It corresponds essentially to quasi-aligned O-Zr-O arrangements inside the ZrO_6 octahedra: the effective scattering amplitude for such types of collinear paths is enhanced by *focusing* effects.[27] These triplet contributions are larger than any other second shell contribution (Fig. 5). The intensity of this feature precludes any significant distortion of the ZrO_6 octahedra.

The high frequency residual in Fig. 5 most probably originates from three-body contributions that were neglected (such as Zr-O-Si, Zr-O-B). An attempt to exploit this information using a detailed scattering-path analysis on selected snapshots taken from the MD trajectories is currently under way.

IV. CONCLUSIONS

A detailed description of the short-range order around zirconium cations in silicate glasses has been obtained thanks to a combination of the x-ray absorption spectroscopy with mo-

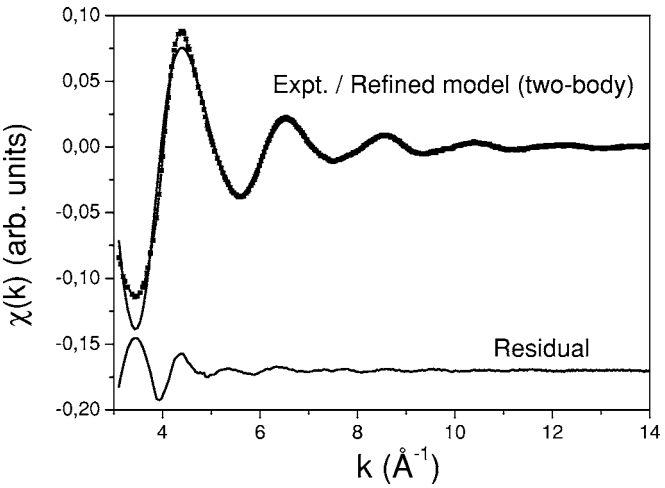

FIG. 4. Comparison of the best-fit signal (solid line) obtained using two-body EXAFS contributions only (ZrO+ZrSi+ZrB +ZrAl) with the experimental spectrum (line+symbol). The residual (dots) is shifted down vertically.

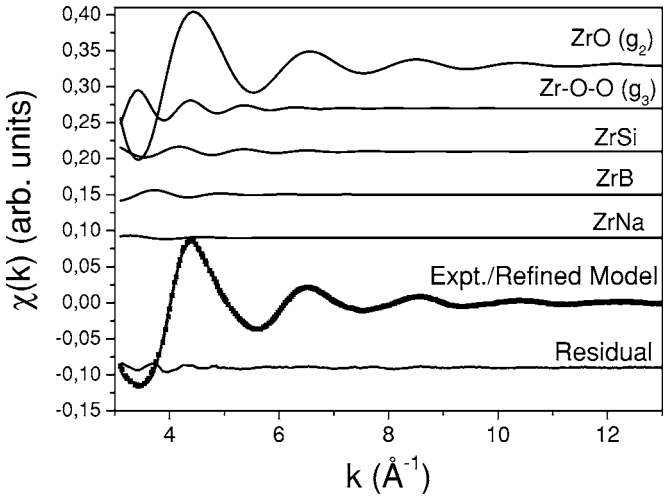

FIG. 5. Comparison of the best-fit signal (solid line) using refined Zr-X (X=O,Si,B,Al,Na) two-body and Zr-O-O three-body EXAFS contributions (shifted up vertically) with the experimental spectrum (line+symbol). The residual (dots) is shifted down vertically.

lecular dynamics simulations. The MD simulations were used to explore the importance of each type of neighbors in the EXAFS signal and to provide a starting model for the EXAFS analysis using the GNXAS package. The experimental information allowed to improve the $g_{ZrO}(r)$ description; the present work thus provides elements for further improvements of the MD parameters used.[28]

The Gaussian-like distribution of the first shell of oxygens reveals a weak radial disorder within the ZrO_6 octahedra. The presence of three-body contributions to the EXAFS signal arising from *intra-octahedra* paths further completes the description of the ZrO_6 octahedra. They indicate a weak angular disorder, as implied by linear O-Zr-O arrangements. The present data are consistent with a Zr cubic O_h symmetry, shown by the absence of splitting of the t_{2g} and e_g final states on Zr $L_{2,3}$ XANES spectra.[10] Previous EXAFS studies of cations (such as, e.g., iron,[29] lead,[30] vanadium[31]) did not evidence such symmetric environments; thus our study indicates a rather specific behavior of Zr.

The presence of n-body correlations with n greater than 2 has often been neglected in the EXAFS analysis of disorded systems (noticeable exceptions can be found, e.g., in Refs. 32 and 33). Their account is, however, crucial in the present case since their contribution is larger than any second neighbor shells. As shown earlier in amorphous silicon,[32] this information allows to access angular distributions and thus paves the way for a better description of the 3D glass structure.

ACKNOWLEDGMENTS

We are grateful to V. Briois and S. Belin for experimental assistance on the D44 beamline at the DCI-LURE synchrotron (Orsay, France). G.F. thanks F. Farges for interesting discussions.

[1] G. Pucker, K. Gatterer, H. P. Fritzer, M. Bettinelli, and M. Ferrari, Phys. Rev. B **53**, 6225 (1996).
[2] P. H. Gaskell, *Models for the Structure of Amorphous Solids* (VCH, Weinheim, 1991), Vol. 9, p. 175.
[3] G. N. Greaves, Miner. Mag. **64**, 441 (2000).
[4] L. Galoisy, L. Cormier, S. Rossano, A. Ramos, G. Calas, P. H. Gaskell, and M. Le Grand, Miner. Mag. **64**, 409 (2000).
[5] C. Meneghini, A. F. Gualtieri, and C. Siligardi, J. Appl. Crystallogr. **32**, 1090 (1999); C. Meneghini, S. Mobilio, L. Lusvarghi, F. Bondioli, A. M. Ferrari, T. Manfredini, and C. Siligardi, *ibid.* **37**, 890 (2004).
[6] L. Barbieri, A. Corradi, I. Lancelloti, C. Leonelli, and C. Siligardi, J. Mater. Sci. **38**, 2627 (2003).
[7] M. B. Wolf, in *Glass Science and Technology* (Elsevier, Amsterdam, 1984), Vol. 7, p. 306.
[8] D. R. Ulhmann and N. J. Kreidl, *Glass Science and Technology. 1. Glass-Forming Systems* (Academic, Cambridge, 1983).
[9] F. Farges, C. W. Ponader, and G. E. Brown, Jr., Geochim. Cosmochim. Acta **55**, 1563 (1991); F. Farges, G. E. Brown, Jr., and D. Velde, Am. Mineral. **79**, 838 (1994); F. Farges and S. Rossano, Eur. J. Mineral. **12**, 1093 (2000).
[10] L. Galoisy, E. Pélegrin, M.-A. Arrio, P. Ildefonse, and G. Calas, J. Am. Ceram. Soc. **82**, 2219 (1999).
[11] D. A. McKeown, I. S. Muller, A. C. Buechele, and I. L. Pegg, J. Non-Cryst. Solids **258**, 98 (1999).
[12] L. Cormier, D. Ghaleb, J.-M. Delaye, and G. Calas, Phys. Rev. B **61**, 14495 (2000); J.-M. Delaye, L. Cormier, D. Ghaleb, and G. Calas, J. Non-Cryst. Solids **293–295**, 290 (2001).
[13] J.-M. Delaye and D. Ghaleb, Phys. Rev. B **61**, 14481 (2000).
[14] J.-M. Delaye and D. Ghaleb, J. Non-Cryst. Solids **195**, 239 (1996); J.-M. Delaye and D. Ghaleb, Mater. Sci. Eng. **B37**, 232 (1996); J.-M. Delaye, V. Louis-Achille, and D. Ghaleb, J. Non-Cryst. Solids **210**, 232 (1997).
[15] M. Montorsi, C. Leonelli, M. C. Menziani, J. Du, and A. N. Cormack, Phys. Chem. Glasses **43**, 137 (2002).
[16] L. Barbieri, V. Cannillo, C. Leonelli, M. Montorsi, P. Mustarelli, and C. Siligardi, J. Phys. Chem. B **107**, 6519 (2003).
[17] A. Filipponi, A. Di Cicco, T. A. Tyson, and C. R. Natoli, Solid State Commun. **78**, 265 (1991); A. Filipponi and A. Di Cicco, TASK Q. **4**, 575 (2000).
[18] A. Filipponi, A. Di Cicco, and C. R. Natoli, Phys. Rev. B **52**, 15122 (1995); A. Filipponi and A. Di Cicco, Phys. Rev. B **52**, 15135 (1995).
[19] A. Filipponi and A. Di Cicco, Phys. Rev. A **52**, 1072 (1995).
[20] R. Newell, B. Feuston, and S. Garofalini, J. Mater. Res. **4**, 434 (1989); H. Melman and S. Garofalini, J. Non-Cryst. Solids **134**, 107 (1991).
[21] A. Filipponi, J. Phys.: Condens. Matter **13**, R23 (2001).
[22] G. Ferlat, J.-C. Soetens, A. San Miguel, and P. A. Bopp, J. Phys.: Condens. Matter **17**, S145 (2005).
[23] P. D'Angelo, A. Di Nola, A. Filipponi, N. V. Pavel, and D. Roccatano, J. Chem. Phys. **100**, 985 (1994).

[24] A. Filipponi, J. Phys.: Condens. Matter **6**, 8415 (1994).
[25] A. Trapananti and A. Di Cicco, Phys. Rev. B **70**, 014101 (2004).
[26] Note that the refinement of all types of contributions (two- and three-body) is done simultaneously. The inclusion of the Zr-O-O three-body contribution, however, did not significantly affect the obtained $g_{ZrO}(r)$ first peak.
[27] P. A. Lee, P. H. Citrin, P. Eisenberger, and B. M. Kincaid, Rev. Mod. Phys. **53**, 769 (1981).
[28] The failure of the MD simulations to reproduce the symmetric shape of the $g_{ZrO}(r)$ first peak might have a *structural* or *chemical* origin: it might be due to inaccuracies in the parameters defining the Zr-O interaction or to a too pronounced chemical disorder of the second neighbors of Zr. If, for instance, the network formers linked with the ZrO_6 were all silicon (or boron) atoms, the $g_{ZrO}(r)$ first peak might be more symmetric. The formation of such chemically ordered environments could be prevented by the short simulations times accessible by MD. Unfortunately, the contribution of subsequent shells (ZrSi, ZrB) in the EXAFS experimental data, although discernible, is small and the question whether enriched domains of either type of network-former cations (Si, B) exist or not cannot be answered by the present study.
[29] S. Rossano, A. Ramos, J.-M. Delaye, S. Creux, A. Filipponi, C. Brouder, and G. Calas, Europhys. Lett. **49**, 597 (2000).
[30] J. Rybicki, A. Rybicka, A. Witkowska, G. Bergmański, A. Di Cicco, M. Minicucci, and G. Mancini, J. Phys.: Condens. Matter **13**, 9781 (2001).
[31] G. Giuli, E. Paris, J. Mungall, C. Romano, and D. Dingwell, Am. Mineral. **89**, 1640 (2004).
[32] A. Filipponi, F. Evangelisti, M. Benfatto, S. Mobilio, and C. R. Natoli, Phys. Rev. B **40**, 9636 (1989); A. Filipponi, A. Di Cicco, M. Benfatto, and C. R. Natoli, Europhys. Lett. **13**, 319 (1990).
[33] L. Cormier, L. Galoisy, and G. Calas, Europhys. Lett. **45**, 572 (1999).